Enhancement of hole injection and electroluminescence characteristics by a rubbing-induced lying orientation of alpha-sexithiophene

Toshinori Matsushima and Hideyuki Murata

Citation: J. Appl. Phys. **112**, 024503 (2012); doi: 10.1063/1.4735402
View online: http://dx.doi.org/10.1063/1.4735402
View Table of Contents: http://jap.aip.org/resource/1/JAPIAU/v112/i2
Published by the American Institute of Physics.

Enhancement of hole injection and electroluminescence characteristics by a rubbing-induced lying orientation of alpha-sexithiophene

Toshinori Matsushima and Hideyuki Murata[a)]
School of Materials Science, Japan Advanced Institute of Science and Technology, 1-1 Asahidai, Nomi, Ishikawa 923-1292, Japan

(Received 5 January 2012; accepted 9 June 2012; published online 17 July 2012)

The authors find that rubbing a film of alpha-sexithiophene (α-6T) with a nylon cloth induces a change from standing to lying orientations in a film surface region. While current densities of hole-only devices based on 4,4′,4″-tris(*N*-3-methylphenyl-*N*-phenyl-amino)triphenylamine (m-MTDATA) are independent of the rubbing number of α-6T, current densities of hole-only devices based on *N*-*N*′-diphenyl-*N*-*N*′-bis(1-naphthyl)-1,1′-biphenyl-4,4′-diamine (α-NPD) and 4,4′-bis(carbazol-9-yl)-2,2′-biphenyl (CBP) markedly increase (≈42 times at 1 V for the α-NPD devices and ≈236 times at 1 V for the CBP devices) as the rubbing number of α-6T is increased. The increase in current density is ascribed to enhanced hole injection through a −5.28 eV energy level of lying α-6T domains instead of a −4.95 eV energy level of standing α-6T domains and improved overlaps between an electronic cloud of indium tin oxide, π orbitals of lying α-6T molecules, and π orbitals of molecules of α-NPD and CBP at heterojunction interfaces. The rubbing of α-6T is also demonstrated to reduce drive voltages (by ≈40% at 10 mA/cm^2) and increase power conversion efficiency (by ≈26% at 10 mA/cm^2) of organic light-emitting diodes. Finally, half lifetimes are significantly enhanced (4.3 times) at a current density of 50 mA/cm^2.
 [http://dx.doi.org/10.1063/1.4735402]

I. INTRODUCTION

Charge injection and transport processes in organic electronic devices such as organic light-emitting diodes (OLEDs) are key factors affecting their current density-voltage characteristics.[1,2] To reduce driving voltage of OLEDs, high-charge-mobility organic materials have been used[3,4] and device structures having minimized heterojunction energy barriers have been designed.[5,6] Also, doping an organic layer with a strong electron donor or acceptor material is effective due to an increase in electrical conductivity and formation of a quasi-Ohmic contact at organic/electrode interfaces.[7,8] The other way to reduce the power consumption is suggested to be control of an orientation of organic molecules. It is well known that organic films and crystals based on a face-to-face stacked orientation of molecules relative to each other (for example, a herringbone configuration) exhibit favorable charge transport due to an overlap of π orbitals.[9,10] This stacked orientation concept has been frequently used in a research area of organic thin-film transistors to increase charge mobility.[11,12] If a molecular orientation can be controlled in a multilayer OLED, charge injection efficiency at a heterojunction interface as well as bulk charge mobility are enhanced, leading to a reduction in power consumption. For examples of previous reports regarding orientations of organic small molecules, Era *et al.* used homoepitaxial growth of *p*-sexiphenyl (6P) on a rubbed surface to obtain polarized electroluminescence (EL) from an oriented 6P film.[13] Yanagi and Okamoto constructed OLEDs by depositing 6P and additional layers on a KCl (001) surface and transferring the multilayer structure to an indium tin oxide (ITO)-coated substrate.[14] A lying orientation of 6P, deposited at a lower temperature, resulted in a lower drive voltage than a standing orientation. Yokoyama *et al.* demonstrated that planar-shaped long organic molecules in vacuum-deposited amorphous films were oriented parallel to a substrate plane.[15] However, the most of vacuum-deposited organic molecules are generally random and it is still underdeveloped to control an orientation of organic small molecules in solid-state films for device applications, whereas there are many techniques used to align long-chain polymers along a certain direction.[16–18]

Recently, we demonstrated that rubbing a film of alpha-sexithiophene (α-6T) with a nylon cloth induced a change from standing to lying orientations in a film surface region.[19] The lying orientation of α-6T increased current densities of hole-only devices by 42 times at 1 V due to enhanced hole injection from α-6T to *N*-*N*′-diphenyl-*N*-*N*′-bis(1-naphthyl)-1,1′-biphenyl-4,4′-diamine (α-NPD), offering an alternative possibility of manufacturing sophisticated organic electronic devices with low power consumption. The aim of this report is to clarify a mechanism of the enhanced hole injection by combining the previous data (Ref. 19) with our recent data. In this study, we choose three kinds of organic material: 4,4′,4″-tris(*N*-3-methylphenyl-*N*-phenyl-amino)triphenylamine (m-MTDATA), α-NPD, and 4,4′-bis(carbazol-9-yl)-2,2′-biphenyl (CBP) having different ionization energy to fabricate hole-only devices and investigate how the rubbing number of α-6T and hole injection barriers at the interfaces of α-6T/m-MTDTA, α-6T/α-NPD, and α-6T/CBP affect current density-voltage characteristics of the hole-only devices. In addition to the discussion of the hole injection mechanism, we demonstrate that the lying orientation of α-6T caused by the rubbing results in a reduction in voltage and

a)Electronic mail: murata-h@jaist.ac.jp.

increases in power conversion efficiency and operational lifetime of OLEDs based on stacked layers of α-NPD and tris(8-hydroxyquinoline)aluminum (Alq_3).

II. EXPERIMETAL

The chemical structures of organic molecules used in this study are shown in Fig. 1(a). High-purity source materials of α-NPD (Nippon Steel Chemical), CBP (Nippon Steel Chemical), Alq_3 (Nippon Steel Chemical), MoO_3 (Mitsuwa Chemical), LiF (Nacalai Tesque), and Al (Nilaco) were used as received and source materials of α-6T (Aldrich) and m-MTDATA (Luminescence Technology) were purified twice using a temperature-gradient vacuum train sublimation technique prior to use. Fused silica substrates and glass substrates coated with a 150 nm ITO layer having sheet resistance of 10 Ω/sq (SLR grade, Sanyo Vacuum Industries) were cleaned using ultrasonication in acetone, followed by ultrasonication in detergent, pure water, and isopropanol. Then, the substrates were placed in an ultraviolet (UV)-ozone treatment chamber (PL21-200, SEN LIGHT) for 30 min.

Fifteen nm α-6T films were vacuum-deposited on the cleaned fused silica substrates at a deposition rate of 0.1 nm/s under a base pressure of 10^{-5} Pa using a vacuum deposition system (E-200, ALS technology). The resulting film thickness and the deposition rate were controlled with a carefully calibrated quartz crystal microbalance. After the α-6T deposition, the substrates were transferred to an adjacent nitrogen-filled glove box (oxygen and water levels are lower than 1 ppm) and the films were repeatedly rubbed 1, 5, 7, 10, and 15 times using a 3.5 cm-diameter cylindrical vial wound with a dust-free nylon cloth in a given direction. The rubbing was conducted by hand, so that the rubbing condition was not controlled precisely, but the transfer speed and the weight of the vial on the films were roughly 25 cm/s and 500 g, respectively. The films were characterized using an UV/visible (UV-vis) absorption spectrometer (V670, JASCO) and an atomic force microscope (AFM) (VN-8000, KEYENCE) in air.

The structures of the hole-only devices and the OLEDs were glass substrate/ITO anode (150 nm)/rubbed α-6T/α-NPD (100 nm)/MoO_3 (10 nm)/Al cathode (100 nm) and glass substrate/ITO anode (150 nm)/rubbed α-6T/α-NPD (90 nm)/Alq_3 (70 nm)/LiF (0.5 nm)/Al cathode (100 nm), respectively [see the device structures shown in Figs. 1(b) and 1(c)]. After the α-6T layer was vacuum-deposited on the cleaned ITO layer and then rubbed using the similar way mentioned before, the additional layers were vacuum-deposited on top of the rubbed layer to complete the devices. The hole-only devices and the OLEDs without α-6T and rubbing were also fabricated for comparison. The devices were encapsulated using a glass cap and an UV curing epoxy resin together with a dessicant sheet, which absorbs both oxygen and water. All fabrication processes were conducted without exposing the samples to air. The device area was 2.25 mm^2, which was defined as the overlapped area of the ITO layer and the Al layer. The deposition rates were set at 0.1 nm/s (α-6T, m-MTDATA, α-NPD, CBP, and Alq_3), 0.05 nm/s (MoO_3), 0.01 nm/s (LiF), and 0.5 nm/s (Al). The current density-voltage-external quantum efficiency characteristics of the devices were measured using a computer-controlled sourcemeter (2400, Keithley) and an integrating sphere installed with a calibrated silicon photodiode. The luminance and the power conversion efficiency of the OLEDs were measured using a computer-controlled luminance meter (BM-9, TOPCON). The EL spectra of the OLEDs were taken using a photonic multi-channel analyzer (C7473, Hamamatsu). To evaluate the operational stability, the changes in luminance and drive voltage of the OLEDs were recorded with time using a lifetime measurement system (PEL-11OT, COMODO SOLUTIONS) when the devices were continuously operated at a constant dc current density of 50 mA/cm^2. All measurements were conducted at room temperature.

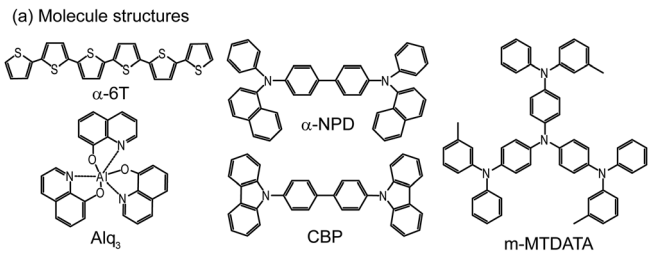

(b) Hole-only device

Al (100 nm)
MoO_3 (10 nm)
m-MTDATA, α-NPD, or CBP (100 nm)
Rubbed α-6T
ITO (150 nm)
Glass substrate

(c) OLED

Al (100 nm)
LiF (0.5 nm)
Alq_3 (70 nm)
α-NPD (90 nm)
Rubbed α-6T
ITO (150 nm)
Glass substrate

FIG. 1. (a) Chemical structures of organic molecules used in this study and schematic structures of (b) hole-only devices and (c) OLEDs.

III. RESULTS AND DISCUSSION

A. Change from standing to lying orientations of α-6T by rubbing

First of all, we discuss the molecular orientation characteristics of the as-deposited and rubbed α-6T films on the fused silica substrates with conventional unpolarized UV-vis absorption spectra, which are measured under light incidence normal (0°) and oblique (45°) to the substrate [Figs. 2(a) and 2(b)]. The absorption in this wavelength range originates from π-π* transition of α-6T having an electronic transition moment along its long molecular axis.[20] There are a strong absorption peak at ≈360 nm and weak vibronic side peaks at 400–600 nm in the as-deposited film. The ≈360 nm peak decreases and the 400–600 nm peaks relatively increase in absorbance after the rubbing. The ≈360 nm peak completely disappears in the films rubbed 10 and 15 times. Egelhaaf *et al.* reported that a thin α-6T film had a sharp blue-shifted absorption peak originating from aggregates of α-6T molecules on a substrate surface.[21] An increase in α-6T thickness reduced the sharp absorption peak and increased the vibronic side absorption peaks in intensity because of reduced molecular order for thicker films. Since the spectral change induced by the rubbing resembles the result of the Egelhaaf's report, the ≈360 nm peak and the 400–600 nm peaks probably arise from aggregated and unaggregated α-6T molecules, respectively. One well-known example of the sharp

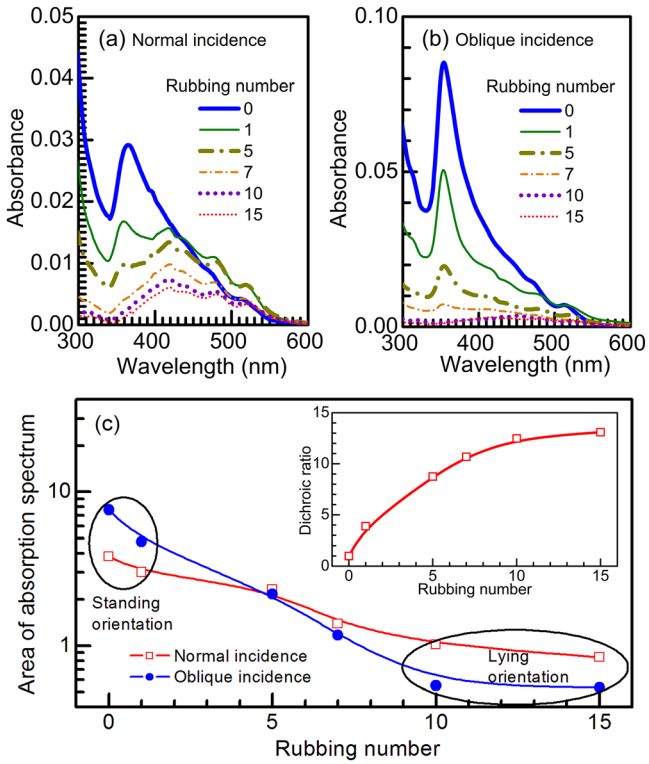

FIG. 2. Unpolarized absorption spectra of as-deposited and rubbed α-6T films measured with (a) normal and (b) oblique light incidence and (c) plots of spectral areas obtained with normal and oblique light incidence versus rubbing number. Inset shows change in absorption dichroic ratio as function of rubbing number when polarized absorption spectra are measured with normal light incidence.

blue-shifted absorption peak is formation of H-aggregates. The disappearance of the ≈360 nm peak in the 10 and 15 times rubbed films means decomposition of aggregated molecules into unaggregated molecules and/or removal of large aggregated molecules with the nylon cloth.

The areas of the unpolarized absorption spectra shown in Figs. 2(a) and 2(b) are calculated in the wavelength range from 300 to 600 nm and plotted versus the rubbing number in Fig. 2(c). The oblique-incidence measurement is expected to increase the areas by $\sqrt{2}$ compared with the normal-incidence measurement because of an increase in path length of light. However, for the as-deposited film, the area obtained with the oblique incidence is about two times larger than that obtained with the normal incidence, indicating that the standing orientation of α-6T is dominant for the as-deposited film because standing molecules can absorb the oblique-incidence light more strongly than the normal-incidence light. It has been reported that the majority of vacuum-deposited α-6T molecules stands on a hydrophilic substrate,[20] which agrees with the result obtained here.

The areas gradually decrease as the rubbing number is increased because of a decrease in film thickness by the rubbing. When the films are rubbed 10 and 15 times, the areas obtained with the oblique incidence become smaller than those obtained with the normal incidence, suggesting that the standing orientation is predominantly changed into the lying orientation. The similar orientation rearrangement has been reported in a rubbed 6P film.[22]

The polarized absorption spectra of the as-deposited and rubbed films were measured under the normal light incidence when an electric field vector of incident light is polarized parallel and perpendicular to the rubbing direction. The data of the absorption dichroic ratios estimated from the polarized spectra are shown in the inset of Fig. 2(c). The absorption dichroic ratio is unity for the as-deposited film, indicating random α-6T molecules in the film plane while the standing α-6T orientation is dominant in the thickness direction. The dichroic ratios gradually increase from 1 to 13 as the rubbing number is increased from 0 to 15. Thus, lying α-6T molecules caused by the rubbing are aligned along the rubbing direction to some extent.

The surface morphology of the as-deposited and rubbed α-6T films are measured using the AFM. The as-deposited film has a relatively smooth surface with small grains [Fig. 3(a)]. After rubbing the films, one can observe an uneven striped texture along the rubbing direction and an increase in surface roughness [Figs. 3(b) and 3(c)], meaning that the films are not rubbed uniformly with the nylon cloth and the lying orientation occurs under the partially rubbed surface regions. The number of the stripes changes and the surface roughness reduces at the larger rubbing number [Figs. 3(d)–3(f)]. Thus, we assume that the lying orientation regions gradually spread on the film surface as the rubbing number is increased.

To investigate a possibility of a rubbing-induced change in electronic state of α-6T, we previously measured photoelectron yield spectra of the as-deposited and rubbed α-6T films using an AC-2 photoelectron yield spectrometer (Riken Keiki).[19] The ionization energy estimated from our photoelectron yield spectra was unchanged between the as-deposited and rubbed films because the rubbed films were too thin (a few nanometer) to detect photoelectrons precisely. Therefore, we prepare thick 50 nm α-6T films on the bare substrate surface and on the 15 times rubbed α-6T surface for the ionization energy measurement. We can confirm from UV-vis absorption spectroscopy that the 50 nm α-6T films on the bare substrate surface and the 15 times rubbed surface mainly include standing and lying α-6T molecules, respectively (this data will be published elsewhere). The ionization energy is calculated to be 4.95 ± 0.02 eV for standing α-6T molecules and 5.28 ± 0.02 eV for lying α-6T molecules from the changes in slope in the photoelectron yield spectra shown in Fig. 4(a), demonstrating that the ionization energy is dependent upon the molecular orientation. It has been reported that a change from standing to lying orientations of α-6T increases its ionization energy,[23] which agrees with our ionization energy results. Thus, two kinds of energy level are probably formed in the rubbed films: one lies on −4.95 eV (originating from standing α-6T molecules) and the other lies on −5.28 eV (originating from lying α-6T molecules).

Based on the results discussed before, we propose the cross sectional structures of the as-deposited and rubbed films as illustrated in Fig. 4(b). Since the films are partially rubbed using the nylon cloth (Fig. 3), four kinds of domain with different electronic states are probably formed in the rubbed films (see Fig. 4(b)):

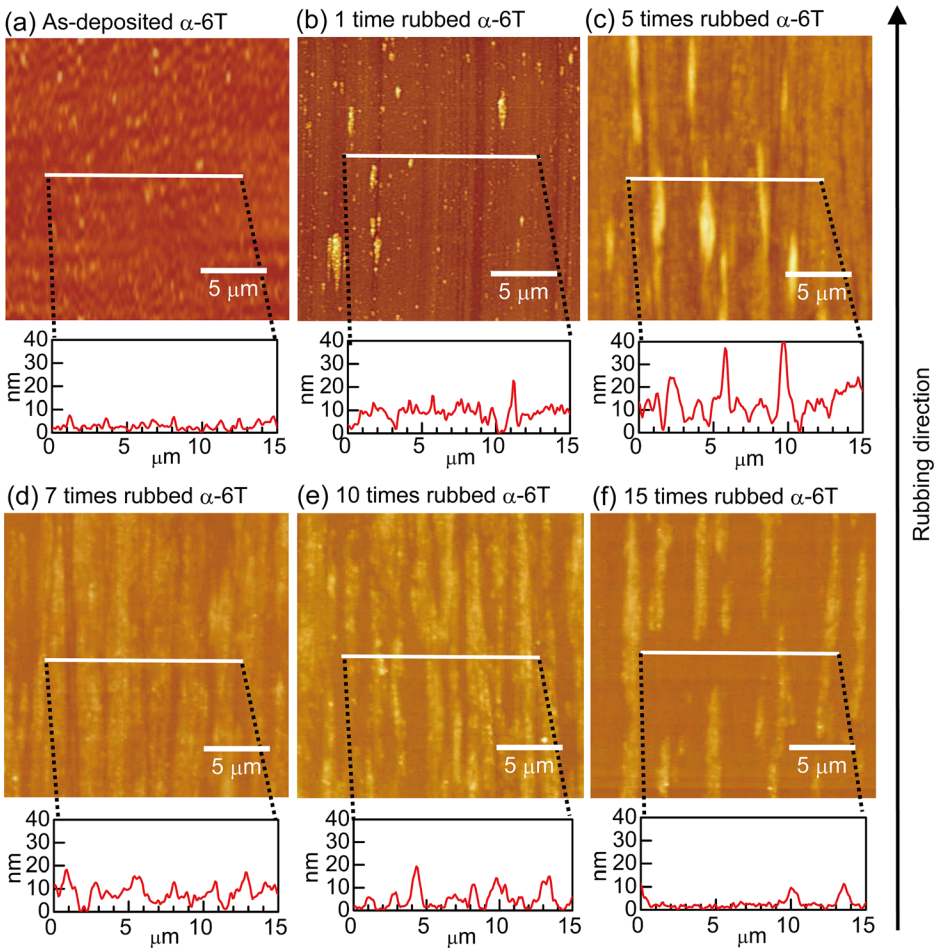

FIG. 3. AFM images and their cross section profiles of (a) as-deposited, (b) 1 time, (c) 5 times, (d) 7 times, (e) 10 times, and (f) 15 times rubbed α-6T films.

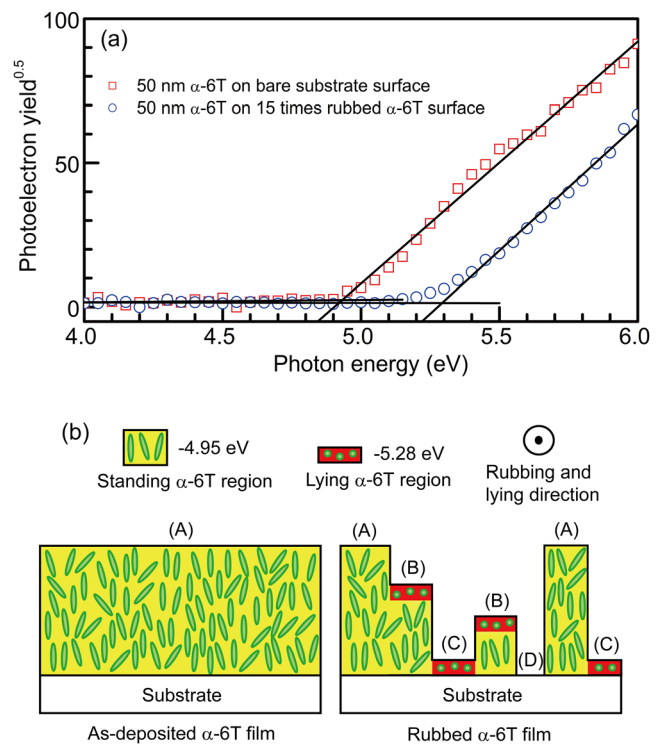

FIG. 4. (a) Photoelectron yield spectra (electrons per incident photons) of 50 nm α-6T films on bare substrate surface and 15 times rubbed α-6T surface and (b) illustrations of proposed molecular orientations for as-deposited and rubbed α-6T films.

(A) Standing α-6T domain: In the domains, surfaces of which are not in contact with the rubbing cloth, standing α-6T molecules are kept intact. Therefore, the standing α-6T domains have the −4.95 eV energy level.
(B) Standing/lying α-6T domain: In the domains, surfaces of which are partially shaved with the rubbing cloth, the domains of this sort have a bilayer orientation structure, where a thin layer of lying α-6T molecules with the −5.28 eV energy level resides on an intact layer of standing α-6T molecules with the −4.95 eV energy level.
(C) Lying α-6T domain: In the domains, surfaces of which are mostly shaved with the rubbing cloth, a thin layer of lying α-6T molecules with the −5.28 eV energy level is only left on the substrate.
(D) Bare substrate domain: In the domains, all α-6T molecules are removed from the substrate with the rubbing cloth, resulting in appearance of a bare substrate surface.

The as-deposited film only contains the homogeneous domains of standing α-6T molecules having the −4.95 eV energy level [(A) standing α-6T domain]. On the other hand, the four domains of (A) standing α-6T, (B) standing/lying α-6T, (C) lying α-6T, and (D) bare substrate coexist in the rubbed films. As the rubbing number is increased, the domains (B), (C), and (D) gradually increase in the films, affecting the current density-voltage characteristics of the hole-only devices and the OLEDs presented later because

the −5.28 eV energy level is more favorable for hole injection than the −4.95 eV energy level.

B. Enhanced hole injection caused by molecular orientation

The hole-only devices with the different rubbing number and organic layers were fabricated to discuss how the molecular orientation of α-6T affects hole injection and transport characteristics [see the device structure shown in Fig. 1(b)]. The 10 nm MoO_3 layer was inserted between α-NPD and Al to prevent electron injection from Al because MoO_3 has a high work function of 5.68 eV.[24] In fact, we did not observe EL from the devices, indicating that hole currents dominate the current density-voltage characteristics. We prepared 8–12 devices on different substrates using separate fabrication processes. The representative current density-voltage characteristics of the hole-only devices are shown in Figs. 5(a), 6(a), and 7(a). The obtained current densities at 0.1, 1, and 4 V are averaged and plotted versus the rubbing number in Figs. 5(b), 6(b), and 7(b). The small margin of error for the current densities indicates good reproducibility. We previously confirmed that the exposure of the devices to a pure nitrogen atmosphere during the rubbing did not degrade the current density-voltage characteristics.[19] The work function of ITO and the ionization energy of m-MTDATA, α-NPD, and CBP were, respectively, measured to be 5.02, 5.06, 5.40, and 5.96 eV using the AC-2 photoelectron yield spectrometer. The energy-level diagrams of the hole-only devices with these values and the two energy levels of α-6T discussed before are depicted in the insets of Figs. 5(a), 6(a), and 7(a).

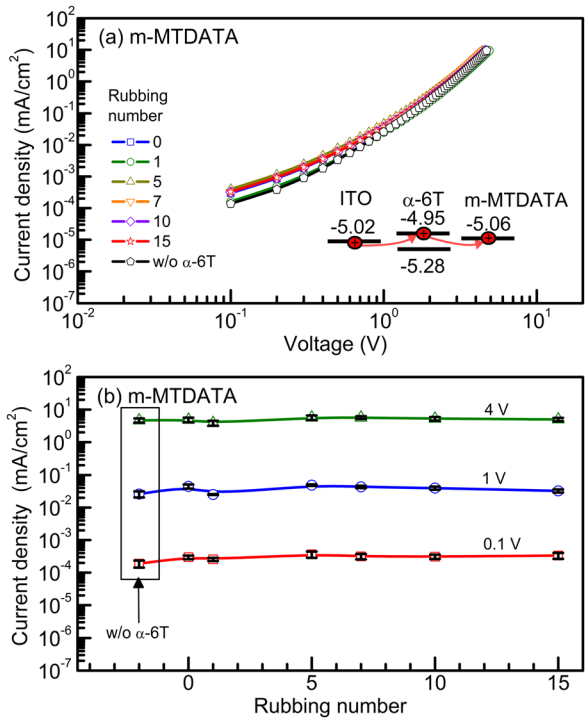

FIG. 5. (a) Current density-voltage characteristics and (b) plots of current densities at 0.1, 1, and 4 V as function of rubbing number for hole-only m-MTDATA devices. Inset shows energy-level diagram of hole-only m-MTDATA devices.

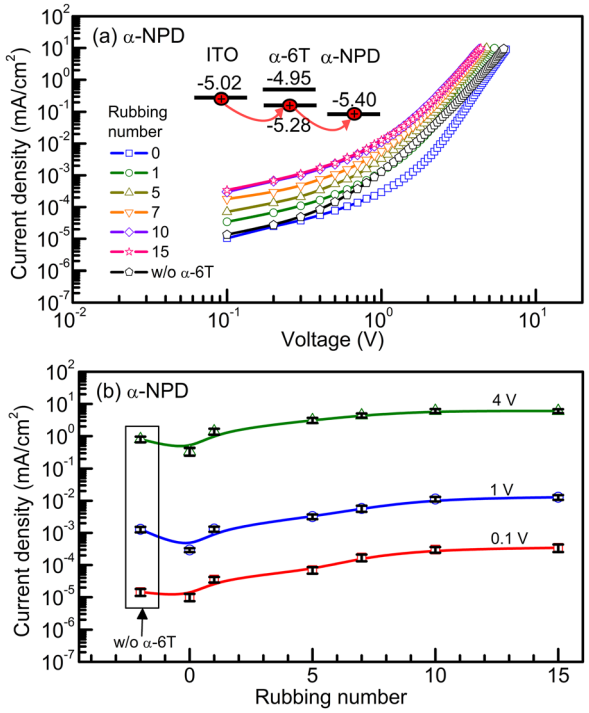

FIG. 6. (a) Current density-voltage characteristics and (b) plots of current densities at 0.1, 1, and 4 V as function of rubbing number for hole-only α-NPD devices. Inset shows energy-level diagram of hole-only α-NPD devices.

When the small-ionization-energy material of m-MTDATA is used, the current density-voltage characteristics are independent of the rubbing number [Figs. 5(a) and 5(b)]. If hole injection occurs though the domains of standing/lying

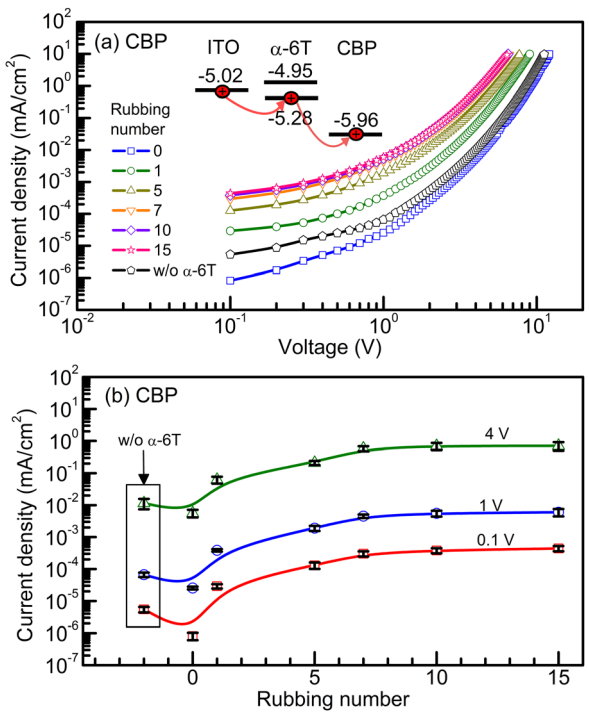

FIG. 7. (a) Current density-voltage characteristics and (b) plots of current densities at 0.1, 1, and 4 V as function of rubbing number for hole-only CBP devices. Inset shows energy-level diagram of hole-only CBP devices.

α-6T (B) and lying α-6T (C), the current densities of the rubbed devices are likely to decrease, but the obtained result is different. Since the Fermi level of ITO (−5.02 eV) and the hole transport levels of standing α-6T (−4.95 eV) and m-MTDATA (−5.06 eV) are close to each other, holes are probably injected from ITO to m-MTDATA through the −4.95 eV hole transport level of the narrowly residual standing α-6T domains (A) [the inset of Fig. 5(a)] or injected directly from the bare ITO domains (D), resulting in the rubbing-independent current density-voltage characteristics.

For the α−NPD devices, the current densities of the unrubbed device are lower than those of the device without α-6T perhaps because of an increased hole-injection barrier at the α-6T/α-NPD interface [the inset of Fig. 6(a)], but we find that the current densities increase (≈42 times at 1 V) as the rubbing number is increased from 0 to 15 [Figs. 6(a) and 6(b)]. Since the current densities of the 15 times rubbed device are higher than those of the device without α-6T, the reduction in α-6T thickness caused by the rubbing is not the major factor for the increased current densities. It has been reported that a hole mobility of α-6T is measured to be 10^{-4}–10^{-2} cm^2/V s using a thin-film transistor structure,[25] which is presumably higher than that of α-NPD (10^{-4}–10^{-3} cm^2/V s) measured using a time-of-flight technique,[26] suggesting that the bulk hole transport (the hole mobility) of α-6T therefore does not limit the current density-voltage characteristics.

The −5.28 eV hole transport level of the lying α-6T domains (C) is more favorable for hole injection than the −4.95 eV hole transport level of the standing α-6T domains (A) because the −5.28 eV hole transport level is intermediate between the Fermi level of ITO (−5.02 eV) and the hole transport level of α-NPD (−5.40 eV). We assume that the hole transport sites in the α-6T layer shift from the standing α-6T domains (A) to the lying α-6T domains (C) and the area of the lying α-6T domains (C) increases gradually as the rubbing number is increased, resulting in the increased current densities. It is possible that improved overlaps between an electronic cloud of ITO, π orbitals of lying α-6T molecules, and π orbitals of α-NPD molecules at the heterojunction interfaces increase the current densities as well. The hole injection via the standing/lying α-6T domains (B) and the bare ITO domains (D) are not probable for the rubbed α-NPD devices because the hole injection of these sorts are energetically unfavorable.

For the CBP devices, we obtain the similar-shaped current density-voltage and current density-rubbing number characteristics to those of the α-NPD devices [Figs. 7(a) and 7(b)] because of the enhanced hole injection via the −5.28 eV hole transport level of the lying α-6T domains (C) and the improved overlaps between an electronic cloud of ITO, π orbitals of lying α-6T molecules, and π orbitals of CBP molecules at the heterojunction interfaces as discussed before. Since there is the larger hole injection barrier at the α-6T/CBP interface than that at the α-6T/α-NPD interface for the unrubbed devices [the insets of Figs. 6(a), and 7(a)], the current density-voltage characteristics of the unrubbed CBP device must be limited by the hole injection process from α-6T to CBP more strongly than that from α-6T to α-NPD. Therefore, the current enhancement ratio of the CBP devices (≈236 at 1 V) would be much larger than that of the α-NPD devices (≈42 at 1 V). From these results, it is obvious that the rubbing-induced lying orientation enhances charge injection more effectively when a charge injection barrier height is larger.

Alternatively, changes in orientation and crystallinity of m-MTDATA, α-NPD, and CBP on the rubbed α-6T surface are likely to occur and affect their hole mobility and hole transport levels. Polarized absorption spectra of 10 nm films of m-MTDATA, α-NPD,[19] and CBP on the 15 times rubbed α-6T surface were measured with the normal and oblique light incidence to investigate their molecule orientation characteristics. No absorption dichroisms were observed from all films, indicating that these molecules are optically random and the molecular orientations in the bulk layers do not occur significantly on the rubbed surface.

We have previously demonstrated that current density-voltage characteristics of the hole-only α-NPD devices are independent of the rubbing number when ITO and Al are reversely wired as a cathode and an anode, respectively (namely, a negative bias).[19] The similar rubbing-independent current density-voltage characteristics were obtained from the negative biased hole-only devices of m-MTDATA and CBP. The rubbing-independent current density-voltage characteristics suggest that the hole mobility of m-MTDATA, α-NPD, and CBP in these bulk layers are not changed significantly. Thus, we can conclude that the enhanced hole injection by the formation of lying α-6T molecules and the improved overlaps between an electronic cloud of ITO, π orbitals of lying α-6T molecules, and π orbitals of molecules of α-NPD and CBP are more essential for the increased current densities than the increase in hole mobility. However, we still cannot rule out the possibility of the changes in orientation and crystallinity of m-MTDATA, α-NPD, and CBP especially near the rubbed α-6T surface, which also affect their hole transport levels and the current density-voltage characteristics. There is room for further investigation on the electronic states proposed here, so that we are now investigating the electronic states of the stacked films in more detail using ultraviolet photoelectron spectroscopy.

C. Improved performance of OLEDs with rubbed α-6T layers

We demonstrate the improvement of the OLED characteristics using the rubbing-induced lying α-6T orientation. The current density-voltage characteristics of the OLEDs are shown in Figs. 8(a) (linear-linear scale) and 8(b) (logarithmic-linear scale). For easy to understand, the current densities at 3, 5, and 8 V and the drive voltages at 1, 10, and 100 mA/cm^2 are plotted together versus the rubbing number [Fig. 8(c)]. We find that the current density-voltage characteristics of the OLEDs [Fig. 8(a)] are changed in the manner similar to those of the hole-only α-NPD devices [Fig. 6(a)], indicating that the increase in current density of the OLEDs is attributed to the enhanced hole injection by the formation of lying α-6T molecules and the improved overlaps between an electronic cloud of ITO, π orbitals of lying α-6T

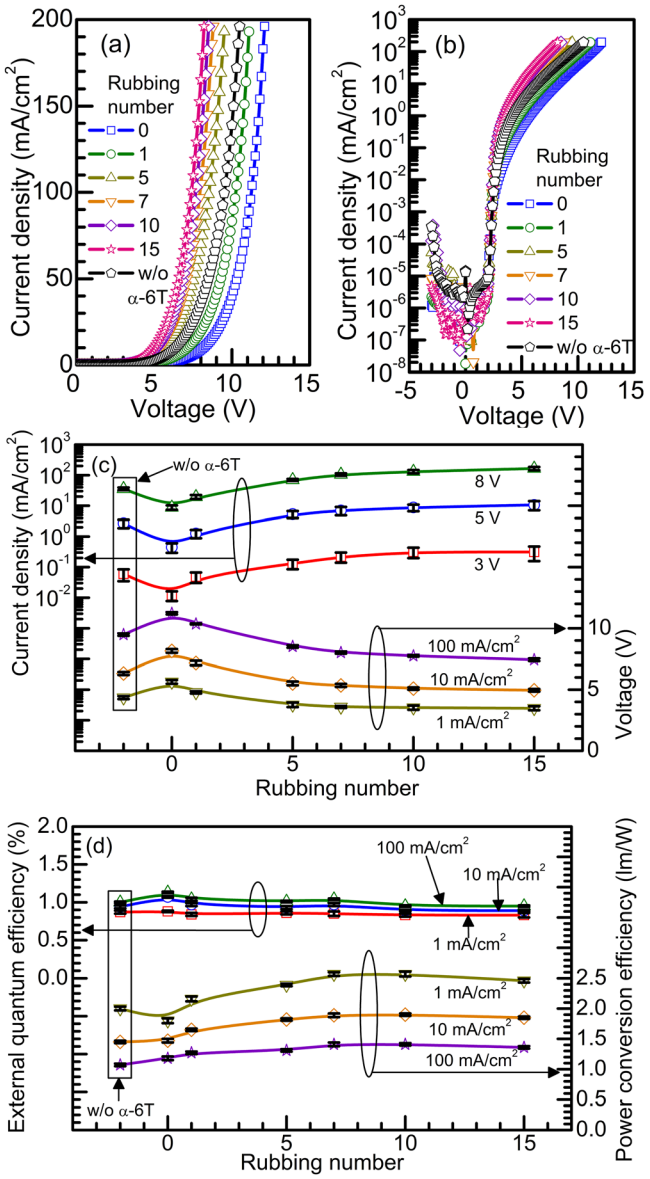

FIG. 8. Current density-voltage characteristics [(a) linear-linear scale and (b) logarithmic-linear scale] and plots of (c) current densities at 3, 5, and 8 V, (c) drive voltages at 1, 10, and 100 mA/cm^2, (d) external quantum efficiency at 1, 10, and 100 mA/cm^2, and (d) power conversion efficiency at 1, 10, and 100 mA/cm^2 as function of rubbing number for unrubbed and rubbed OLEDs.

molecules, and π orbitals of α-NPD molecules. It is likely that the increase in surface roughness after the rubbing (Fig. 3) results in an unexpected leakage current through the OLEDs, but no significant leakage current is observed in a low voltage region less than 2 V [Fig. 8(b)] probably because of very good coverage of the rubbed surfaces with α-NPD and Alq_3. The current densities increase (≈24 times at 5 V) and the drive voltages decrease (by ≈40% at 10 mA/cm^2) as the rubbing number is increased from 0 to 15 [Fig. 8(c)]. Besides the hole injection from ITO to α-NPD through α-6T and the hole transport in α-NPD, the processes of electron transport in Alq_3, electron injection from LiF/Al to Alq_3, and hole injection from α-NPD to Alq_3 limit the current density-voltage characteristics of the OLEDs to some extent. Therefore, the current enhancement ratio of the OLEDs (≈24 at 5 V) would be smaller than that of the hole-only α-NPD devices (≈42 at 1 V). The drive voltages of the OLED without α-6T are comparable to those of previously reported OLEDs based on α-NPD and Alq_3.[27,28]

We obtained similar EL spectra from every OLED, which originate from electrically excited Alq_3. The external quantum efficiency is not changed significantly in comparison with the drive voltages and the power conversion efficiency, but slightly decrease (by ≈17% at 10 mA/cm^2) at the larger rubbing number [Fig. 8(d)] because of an excess number of injected holes in the Alq_3 layer[29] and/or exciton quenching by accumulated holes at the α-NPD/Alq_3 interface.[30] On the other hand, the power conversion efficiency increases by the rubbing (by ≈26% at 10 mA/cm^2) [Fig. 8(d)] because the decrease in voltage overcomes the decrease in external quantum efficiency. The shapes and the peaks (525 ± 5 nm) of the EL spectra and the external quantum efficiency values (≈1%) are in good agreement with those of previously reported OLEDs with an Alq_3 emitter.[31–33]

The operational stability of the OLEDs is markedly dependent upon the rubbing number. The luminance/initial luminance-time and voltage-time characteristics of the OLEDs are shown in Figs. 9(a) and 9(b). The initial luminance at the operation current density of 50 mA/cm^2 is about 1500 cd/m^2, which slightly depends on the rubbing number. The half lifetimes and the voltage increase rates are, respectively, defined as the time at which the luminance reduced to half of their initial luminance and the slopes between the initial and last data points. The half lifetimes and the voltage increase rates are plotted as a function of the rubbing number in Fig. 9(c). The larger rubbing number makes it possible to increase the half lifetimes and suppress the voltage increase rates. The half lifetime of the 15 times rubbed OLED is 4.3 times longer than that of the unrubbed OLED. This is the first demonstration of the enhanced OLED lifetimes by controlling the molecular orientation.

Operating OLEDs under a higher voltage at a higher temperature accelerates degradation of OLEDs, indicating that device degradation rapidly proceeds under the high temperature condition.[34,35] The reduction in voltage caused by the rubbing reduces a temperature increase inside the OLEDs, perhaps suppressing generation of nonradiative recombination centers and/or luminance quenchers in a carrier recombination zone. The photoluminescence (PL) spectra from the Alq_3 layers inside the fresh and operated OLEDs were measured using the C7473 analyzer with an excitation light wavelength of 425 nm, where α-NPD absorption is negligible, but weak Alq_3 absorption is still present. We obtained a reduction in PL intensity of Alq_3 by ≈19% in all OLEDs. Since the 425 nm light excites the whole Alq_3 layer in the thickness direction, it is probable that PL intensity in a thin carrier recombination zone near the α-NPD/Alq_3 interface is smaller than ≈19% obtained here. The observed reduction in PL intensity is indicative of generation of nonradiative recombination centers and/or luminance quenchers in the Alq_3 layers. Nevertheless, the detailed reason of the enhanced lifetimes observed here has not yet been understood to date, and so is under investigation now. Finally, we would like to stress that our rubbing technique surely

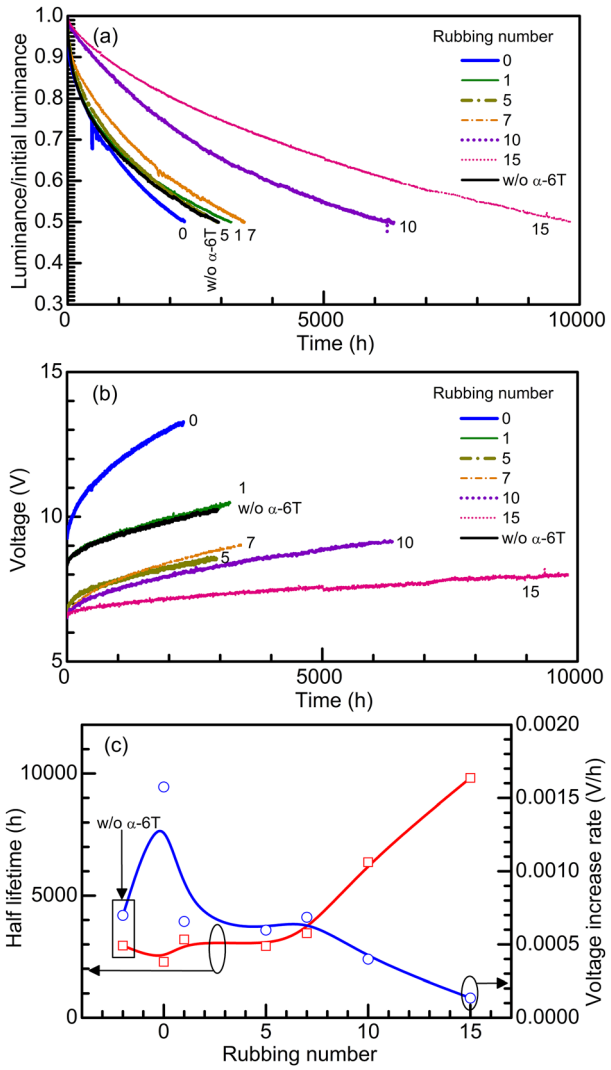

FIG. 9. (a) Luminance/initial luminance-time and (b) drive voltage-time characteristics and (c) plots of half lifetimes and voltage increase rates for unrubbed and rubbed OLEDs. Devices were operated under constant current density of 50 mA/cm^2.

reduces the drive voltages and increases the power conversion efficiency and the long-term stability of the OLEDs, which are useful for practical applications.

IV. CONCLUSIONS

From results of absorption spectra and AFM images, we find that rubbing an α-6T film with a nylon cloth induces a change from standing to lying orientations in partially rubbed film surface regions and the lying orientation regions gradually spread through the film as rubbing number is increased. In the rubbed α-6T film, two kinds of energy level are probably formed: one lies on −4.95 eV (originating from standing α-6T molecules) and the other lies on −5.28 eV (originating from lying α-6T molecules). Hole-only devices based on m-MTDATA, α-NPD, and CBP are fabricated on the rubbed α-6T surfaces to investigate how the molecular orientation of α-6T affects their current density-voltage characteristics. While current densities of the m-MTDATA devices are independent of the rubbing number, current densities of the α-NPD and CBP devices markedly increase (≈42 times at 1 V for the α-NPD devices and ≈236 times at 1 V for the CBP devices) as the rubbing number of α-6T is increased. The increased current densities are ascribed to enhanced hole injection through the −5.28 eV energy level of lying α-6T domains instead of the −4.95 eV energy level of standing α-6T domains as well as and improved overlaps between an electronic cloud of ITO, π orbitals of lying α-6T molecules, and π orbitals of molecules of α-NPD and CBP at heterojunction interfaces. We also find that the rubbing of the α-6T layer reduces drive voltages (by ≈40% at 10 mA/cm^2) and increases power conversion efficiency (by ≈26% at 10 mA/cm^2) and half lifetimes (4.3 times at 50 mA/cm^2) of OLEDs because of the lying α-6T orientation.

A multilayer structure has been widely used in OLEDs and organic solar cells (OSC) to improve their electron-to-photon and photon-to-electron conversion efficiency. Although there have been some reports regarding a naturally formed lying orientation of organic molecules in a vacuum-deposited film,[10,15] organic molecules in each layer of the standard multilayer devices are generally random. The lying molecular orientation demonstrated here occurs only in the very thin α-6T layer, but the improvement of the device performances caused by the lying α-6T orientation is significant. If multilayer devices having lying orientations of organic molecules in each layer can be realized, excellent charge injection, transport, and collection characteristics will be obtained. The lying orientation is also useful to increase light out-coupling efficiency of OLEDs (Ref. 36) and light-harvesting efficiency of OSCs.[37] We are currently aiming at fabricating such lying orientation devices by homo- and hetero-epitaxially growing several kinds of organic layer on the rubbed surface.

ACKNOWLEDGMENTS

The authors are grateful to Grants-in-Aid for Scientific Research of Japan (Grant Nos. 21760005, 20241034, and 20108012) for financial support. This research is supported by the Japan Society for the Promotion of Science (JSPS) through its "Funding Program for World-Leading Innovative R&D on Science and Technology (FIRST Program)."

[1]I. D. Parker, J. Appl. Phys. **75**, 1656 (1994).
[2]A. P. Kulkarni, C. J. Tonzola, A. Babel, and S. A. Jenekhe, Chem. Mater. **16**, 4556 (2004).
[3]S.-J. Su, T. Chiba, T. Takeda, and J. Kido, Adv. Mater. **20**, 2125 (2008).
[4]Y. Sun, L. Duan, D. Zhang, J. Qiao, G. Dong, L. Wang, and Y. Qiu, Adv. Funct. Mater. **21**, 1881 (2011).
[5]S. Tokito, K. Noda, and Y. Taga, J. Phys. D: Appl. Phys. **29**, 2750 (1996).
[6]T. Matsushima and C. Adachi, Appl. Phys. Lett. **92**, 063306 (2008).
[7]F. Huang, A. G. MacDiarmid, and B. R. Hsieh, Appl. Phys. Lett. **71**, 2415 (1997).
[8]J. Huang, M. Pfeiffer, A. Werner, J. Blochwitz, and K. Leo, Appl. Phys. Lett. **80**, 139 (2002).
[9]V. C. Sundar, J. Zaumseil, V. Podzorov, E. Menard, R. L. Willett, T. Someya, M. E. Gershenson, and J. A. Rogers, Science **303**, 1644 (2004).
[10]D. Yokoyama, Y. Setoguchi, A. Sakaguchi, M. Suzuki, and C. Adachi, Adv. Funct. Mater. **20**, 386 (2010).
[11]D. J. Gundlach, T. N. Jackson, D. G. Schlom, and S. F. Nelson, Appl. Phys. Lett. **74**, 3302 (1999).
[12]K. Takimiya, H. Ebata, K. Sakamoto, T. Izawa, T. Otsubo, and Y. Kunugi, J. Am. Chem. Soc. **128**, 12604 (2006).
[13]M. Era, T. Tsutsui, and S. Saito, Appl. Phys. Lett. **67**, 2436 (1995).

[14]H. Yanagi and S. Okamoto, Appl. Phys. Lett. **71**, 2563 (1997).
[15]D. Yokoyama, A. Sakaguchi, M. Suzuki, and C. Adachi, Appl. Phys. Lett. **93**, 173302 (2008).
[16]J. C. Wittmann and P. Smith, Nature (London) **352**, 414 (1991).
[17]M. Grell and D. D. C. Bradley, Adv. Mater. **11**, 895 (1999).
[18]H. Sirringhaus, R. J. Wilson, R. H. Friend, M. Inbasekaran, W. Wu, E. P. Woo, M. Grell, and D. D. C. Bradley, Appl. Phys. Lett. **77**, 406 (2000).
[19]T. Matsushima and H. Murata, Appl. Phys. Lett. **98**, 253307 (2011).
[20]D. Oelkrug, H.-J. Egelhaaf, and J. Haiber, Thin Solid Films **284–285**, 267 (1996).
[21]H.-J. Egelhaaf, P. Bäiuerle, K. Rauer, V. Hoffmann, and D. Oelkrug, Synth. Met. **61**, 143 (1993).
[22]N. Aoki, Y. Koshiba, and Y. Ueda, Jpn. J. Appl. Phys., Part 1 **44**, 4088 (2005).
[23]S. Duhm, G. Heimel, I. Salzmann, H. Glowatzki, R. L. Johnson, A. Vollmer, J. P. Rabe, and N. Koch, Nature Mater. **7**, 326 (2008).
[24]T. Matsushima, Y. Kinoshita, and H. Murata, Appl. Phys. Lett. **91**, 253504 (2007).
[25]X. Peng, G. Horowitz, D. Fichou, and F. Garnier, Appl. Phys. Lett. **57**, 2013 (1990).
[26]S. Naka, H. Okada, H. Onnagawa, Y. Yamaguchi, and T. Tsutsui, Synth. Met. **111–112**, 331 (2000).
[27]S. A. Van Slyke, C. H. Chen, and C. W. Tang, Appl. Phys. Lett. **69**, 2160 (1996).
[28]S.-F. Chen and C.-W. Wang, Appl. Phys. Lett. **85**, 765 (2004).
[29]T. Tsutsui, Mater. Res. Soc. Bull. **22**, 39 (1997).
[30]Y. Luo, H. Aziz, G. Xu, and Z. D. Popovic, Chem. Mater. **19**, 2288 (2007).
[31]T. Dobbertin, M. Kroeger, D. Heithecker, D. Schneider, D. Metzdorf, H. Neuner, E. Becker, H.-H. Johannes, and W. Kowalsky, Appl. Phys. Lett. **82**, 284 (2003).
[32]P.-C. Kao, S.-Y. Chu, Z.-X. You, S. J. Liou, and C.-A. Chuang, Thin Solid Films **498**, 249 (2006).
[33]K. Okumoto, H. Kanno, Y. Hamada, H. Takahashi, and K. Shibata, Appl. Phys. Lett. **89**, 013502 (2006).
[34]I. D. Parker, Y. Cao, and C. Y. Yang, J. Appl. Phys. **85**, 2441 (1999).
[35]X. Zhou, J. He, L. S. Liao, M. Lu, X. M. Ding, X. Y. Hou, X. M. Zhang, X. Q. He, and S. T. Lee, Adv. Mater. **12**, 265 (2000).
[36]J. Frischeisen, D. Yokoyama, A. Endo, C. Adachi, and W. Brütting, Org. Electron. **12**, 809 (2011).
[37]V. Kažukauskas, V. Čyras, M. Pranaitis, C. Sentein, L. Rocha, P. Raimond, I. Duyssens, I. Van Severen, T. Cleij, L. Lutsen, and D. Vanderzande, Thin Solid Films **516**, 8963 (2008).